Molecular dynamics study of the effect of surfactants on droplet deformation in shear flows

W. Li,[1] G. H Ko,[2] and D. Gersappe[1]
[1]*Department of Materials Science and Engineering, SUNY at Stony Brook, Stony Brook, New York 11794, USA*
[2]*MC-RIC, Suite 600, One Broadway, Cambridge, Massachusetts 02142, USA*
(Received 8 July 2005; published 12 December 2005)

We use molecular dynamics simulations to study the effect of surfactants on the mechanism of drop deformation in shear flows. Our results show deviations from fluid mechanics predictions, in both the high and the low surfactant concentration limits. We find that these deviations are a result of the local conformation of the surfactant layer which mediates the stress transfer across the interface. We show that the ability of the surfactant to affect the stress transfer across the interface is a result of the interplay between the architecture of the surfactant and the surface coverage.

DOI: 10.1103/PhysRevE.72.066305 PACS number(s): 47.55.Dz, 36.20.Ey, 82.70.Uv

The mechanisms controlling droplet deformation and breakup in the presence of surfactants, though critical to processes as varied as oil recovery, food processing and multiphase polymer blend production, are still not understood [1–3]. Fluid mechanics theories predict that the process is controlled by the gradients in interfacial tension that result from the redistribution of surfactants on the drop surface by the external flow field [4–8]. These theories assume that the only role of the surfactant is to reduce the interfacial tension of the drop. The experimental evidence on this score, however, is contradictory; for though there are some experiments that support fluid mechanics assumptions [9,10], there are others which indicate that the surfactant participates in the deformation process by altering the interfacial rheology [11–14]. In this paper, we examine this contradiction by using a simulation that studies the process at a molecular level. We show that the role of the surfactant on droplet deformation is not limited to interfacial tension reduction alone. Rather, we find that the local conformation of the surfactant layer (which is controlled by the architecture of the surfactant and the surface coverage) affects the stress transfer across the interface and is key to the deformation process. Since these effects are determined by the molecular structure of the surfactant, fluid mechanics calculations will need to account for such local effects in order to model the system accurately.

Within the explanations that have been postulated to reconcile the points of coincidence and conflict between experiments and existing fluid mechanical theories of drop deformation in the presence of surfactants [9–14], it has been recognized that the interfacial layer between the two phases is key to the deformation process. A fundamental understanding of the process would hence require that the problem be studied at a length scale that is on the order of the size of the interfacial layer. Neither experimental studies (which are limited by difficulties in visualizing the surfactant layer during shear), nor fluid mechanics theories have the necessary detail to study such fine length scales. By using a molecular dynamics (MD) simulation, however, we can follow the trajectory of individual molecules during the deformation process, and isolate the role of the surfactant on the drop deformation process.

In the simulation water and oil molecules are modeled as atomic liquids [15] and the surfactant is modeled using a bead-spring model with a chain length of eight segments [16]. Species of mass m, and separated by a distance r, interact via a generalized Lennard-Jones (LJ) potential of the form $V(r)=4\epsilon[(\sigma/r)^{12}-\delta(\sigma/r)^{6}]$ for $r<r^{c}=2.2\sigma$. Here ϵ and σ are the characteristic energy and length scales, and the potential is zero for $r>r^{c}$. Adjacent monomers along the chain are coupled by an additional potential: $V^{\mathrm{CH}}(r)=-(1/2)kR_0^2\ln[1-(r/R_0)^2]$, for $r<R_0$ where $R_0=1.5\sigma$ and $k=30\epsilon/\sigma^2$. δ is set to 1.0 for same species and is chosen as 0.25 between the water and oil molecules to ensure immiscibility. A planar Couette geometry with the oil drop in the center is used in our simulation. The simulation box is bounded by the walls in the z direction and periodic boundary conditions are applied in x and y directions. Wall atoms are neutral to all other species. All species have the same length scale, energy scale and mass. The density of the fluid system is fixed at 0.81 and the temperature is 1.1 ϵ/kT. The total number of particles is 56 700, with 600 oil atoms in the oil drop and 5760 wall atoms. τ is the characteristic time scale of the simulations defined as $\tau=(m\sigma^2/\epsilon)^{1/2}$. Snapshots of the simulation configuration are shown in Fig. 1, for both the pure drop as well as the surfactant coated drop systems. After equilibration, the top and bottom walls are moved simultaneously in the x direction with opposite velocities $=0.6\sigma/\tau$ to set up an approximately linear shear flow. Constant temperature is maintained by damping the walls and the y component of the velocity of the fluids using a Langevin damping factor. We study the effect of surfactant structure on drop deformation by explicitly modeling two types of surfactants in a water/oil mixture: a homosurfactant (where each

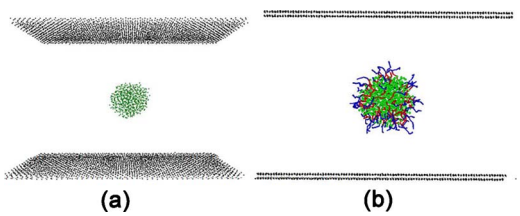

FIG. 1. (Color online) Snapshots of the MD simulation showing the geometry of the system. (a) An oil drop in the center of the simulation box shown in depth view. (b) A xy projection of the system showing the surfactants adsorbed onto the drop. Only the adsorbed surfactants are shown for clarity

TABLE I. Characteristics of the drop system.

Type	Concentration (%)	Surface coverage (monomers/σ^2)	Interfacial Tension (ϵ^2/σ)	Ca	Pe	β
Homo surfactant	0.625	0.40±0.01	1.8±0.1	0.26±0.02	47±10	0.15±0.01
	1.25	0.92±0.05	1.4±0.1	0.38±0.04	62±10	0.35±0.05
Block surfactant	0.625	0.40±0.01	1.9±0.1	0.25±0.02	54±10	0.10±0.01
	1.25	1.06±0.05	1.6±0.2	0.35±0.06	85±30	0.27±0.02

bead is neutral to both oil and water atoms) and a diblock surfactant (consisting of one hydrophilic and one hydrophobic block of equal lengths). Here a homosurfactant is used as a prototype for random copolymer surfactant [17].

The crucial parameters used to characterize the deformation of a drop in fluid mechanics theories are three dimensionless numbers: (i) the capillary number $Ca=\mu_D G/(\gamma/a)$, which defines the ratio between the viscous stresses as a result of the shearing forces and interfacial tension stress on the surface of the droplet (where μ_D is the viscosity of the dispersed phase, γ the interfacial tension of an oil drop in the continuous phase, G the shear rate, and a the drop radius); (ii) the Peclet number $Pe=Ga^2/D_S$, which expresses the relative importance of convection to diffusion (where D_S is the surface diffusion constant of the surfactants), and (iii) the elastic parameter $\beta=-d(\gamma/\gamma_0)/d\theta$, which indicates the sensitivity of interfacial tension to variations in surfactant surface concentration (where γ_0 is the interfacial tension of a drop without surfactants, and θ is the ratio between the surface concentration of surfactant under flow and surface concentration in the absence of flow).

Fluid mechanics theories use the relative magnitude of these numbers to make two main predictions about the process of drop deformation. The first, that in both the soluble and insoluble limits, at lower concentrations of surfactants, when $Pe \gg 1$, the distribution of surfactants on the drop surface is controlled by the parameter β. Thus, at low values of β, there will be an accumulation of surfactants at the ends of the drop in shear or extensional flow [4–8], whereas as β increases, Marangoni stresses due to the interfacial tension gradient will pull the drop fluids and surfactants to the equator of the drop, resulting in a uniform distribution of surfactant over the drop surface [4–8]. The second prediction states that at higher concentrations of surfactants, when the drop is uniformly covered with surfactants, the deformation of the drop will be the same as a surfactant-free drop with an equivalent interfacial tension [7,8].

We use our MD simulation to examine these two predictions by locating our simulation in the same regime as fluid mechanics theories [18]. Our calculations of Pe, Ca, β, and the interfacial tension γ are shown in Table I. As the size of surfactant is much smaller than the size of the drop and it is much simpler to carry out calculations in a planar geometry, these parameters are derived from the surface tension and diffusion constant determined from a planar oil/water interface. The parameters used in our MD simulation are in the same range as experimental and fluid mechanics calculations [18]. We take care to locate ourselves in the $Pe \gg 1$ regime, because it is a theoretical limit that can also be accessed by experiments. To ensure that our simulation is able to recover the same macroscopic behavior as fluid mechanics theories, we consider the limit without any surfactants because it is a limit where there is excellent agreement between fluid mechanics theories and experiments. The deformation ratio D of the oil drop [where $D=(l-b)/(l+b)$, and l and b are the major and minor axes of an elliptically deformed drop] calculated by our simulation agrees well with fluid mechanics calculations over a range of interfacial tensions between the oil and the water phase. For example, a droplet with an interfacial tension of $\gamma=2.16(\epsilon/\sigma^2)$ in the simulation gives $D=0.20\pm0.01$ compared to $D=0.23$ which is calculated from the linear theory of Taylor [19] using the equation $D=35Ca/32$. (Other studies have already established that this simple equation gives excellent agreement over a large range of Ca [20].) This indicates that our system size is large enough to recover the bulk properties of the drop system.

We first study the effect of shear on the surfactant distribution on the surface of the drop at low surfactant concentrations. Surfactants are allowed to adsorb onto or desorb from the drop (soluble limit). In some cases we change nonadsorbed diblock surfactants to water molecules so the total amount of surfactant is fixed and no desorption and adsorption occurs in shear (insoluble limit). In the soluble surfactant limit, we find that the homosurfactant (which has a larger β value) is uniformly distributed on the drop surface, while the diblock surfactant (which has a small β value) accumulates at the ends of the drop, in agreement with the first prediction of the fluid mechanics theories. We quantify this phenomena by plotting the correlation function, $g(r)$, for the adsorbed surfactants in Fig 2. The correlation function $g(r)$ is defined as $g(r)=n(r)/\Sigma n(r)$, where $n(r)$ is defined as the probability that a monomer on a surfactant chain is lo-

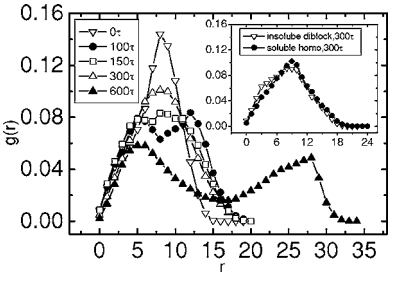

FIG. 2. A plot of the monomer-monomer correlation function $g(r)$ for adsorbed surfactants as a function of r, the distance between monomers, in the low surfactant coverage limit. The main plot shows the time evolution for the soluble diblock surfactant covered drop. The inset shows the steady state $g(r)$ for the insoluble diblock surfactant and the soluble homo-surfactant covered drops.

cated at a distance r away from the monomer of interest, normalized by the sum over all possible pairs in the system. For the homosurfactant covered drop, $g(r)$ shows only a single peak (Fig. 2), confirming that the homosurfactants are always distributed uniformly along the drop surface during the shearing process. For, the diblock surfactant $g(r)$, which starts off as a single peak, splits into two peaks after the shear is applied, the second peak signaling the existence of two surfactant clusters (Fig. 2). In the insoluble surfactant limit, however, we find a discrepancy between our simulations and the fluid mechanics theories. When we fix the total amount of block surfactants at the drop surface by changing all the nonadsorbed surfactants to water molecules, we find that, though the diblock surfactants accumulate at the ends of the drop at the initial stage of shear (below 200 τ), they distribute uniformly over the drop surface at steady state (Fig. 1), in contrast to the prediction of fluid mechanics theories, where one would still expect to see accumulation of surfactants at the ends of the drop. Further, we note that the soluble diblock surfactant covered drop breaks up in the late stages of shear into two drops, while both the insoluble diblock surfactant covered drop and the soluble homosurfactant covered drop do not break up, but reach a steady state deformation. The soluble block surfactant covered drop breaks up at a point at which its deformation ratio D_{sb} is ≈ 0.7, a value larger than the predicted critical deformation ratio (D_c) for break up ($D_c \approx 0.55$). The steady state deformation ratio's for the soluble homosurfactant and the insoluble block surfactant are $D_{sh}=0.38\pm0.01$ and $D_{ib}=0.32\pm0.02$, respectively.

We find that the discrepancies between fluid mechanics theories and our simulations are magnified in the high surfactant concentration limit. Fluid mechanics theories state that, in this limit, the extent of deformation of a surfactant covered drop should be the same as a drop without any surfactants but with the same interfacial tension as the surfactant covered drop (which we henceforth referred to as a "clean" drop). Our simulations, in both the soluble and insoluble surfactant limit, show that both the homosurfactant covered drop and the diblock surfactant covered drop deform much more than the equivalent "clean" drop (Fig. 3).

Our results indicate that the role of the surfactant is not limited to interfacial tension reduction, since surfactants with similar interfacial tensions but with different architectures show qualitatively different behavior (Table I). Yet, what are the other possible mechanisms by which the architecture of the surfactant participates in the deformation process? One possibility is suggested by an analogous polymeric system—the strengthening of the interface between two incompatible polymers by a compatibilizer, which is a high molecular weight surfactant. The compatibilizer serves not only to reduce the interfacial tension, but also to bridge the two phases, thereby acting as a means by which stress is transferred across the interface [21]. Studies of this system have shown that the stress transfer across the interface is affected by the extent to which the compatibilizer penetrates each phase. Equilibrium mean field studies of copolymer adsorption at liquid interfaces have shown that the extent of penetration depends on both the molecular architecture and the concentration of compatibilizer [22]. Extending this analogy

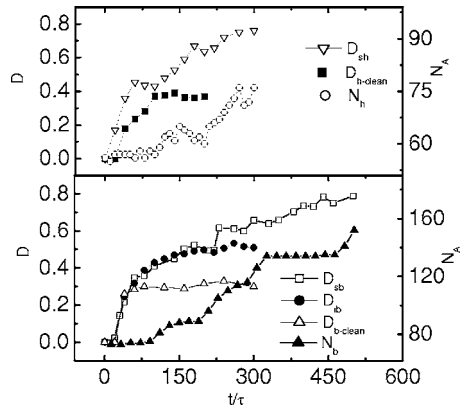

FIG. 3. The top plot shows the deformation ratio D_{sh} for the homosurfactant covered drop, the deformation ratio $D_{h\text{-clean}}$ of the equivalent "clean" drop, and the number of homosurfactants adsorbed N_h on the drop as a function of time. The lower plot shows the deformation ratio of the soluble block surfactant D_{sb}, the deformation ratio D_{isb} for the insoluble block surfactant, the deformation ratio $D_{b\text{-clean}}$ of the equivalent "clean" drop, and the number of block surfactants adsorbed N_b on the drop as a function of time. These plots are in the high surfactant coverage limit.

to our system would suggest that the surfactant, which also bridges the two phases, contributes to the deformation of the drop by improving the momentum transfer between the two phases. This explanation is supported by studies showing that in the absence of surfactant, the interfacial region is characterized by a depletion zone (where there is a local reduction in the density) which reduces the efficiency of momentum transfer between the two phases [23].

To verify our hypothesis, i.e., that the surfactant layer mediates the stress transfer across the interface, we designed a MD simulation for an oil-water-surfactant system with a planar interface. The system is split into a top part (water phase) and a bottom part (oil phase). The system size is the same as the drop system. By moving the walls with the same velocity as in the drop system, a similar velocity field is established. The equilibrium properties of the system (in particular, the width of surfactant layer) at both low and high concentrations of surfactants are shown in Table II. The effects of surfactants on the interfacial rheology can be studied from steady state velocity profiles in shear flow. To quantify our results, we define the "slip" or "stick" length as the distance between the points when the velocity profiles of the oil and water phases are extrapolated to zero. (In the absence of an interface, the velocity at the center of the system is zero.) A slip interface refers to the situation that the slope of veloc-

TABLE II. Characteristics of the planar interface system.

Type	Surface coverage (monomers/σ^2)	Width (σ)	Stick length (σ)
Homosurfactant	0.58 ± 0.02	1.31 ± 0.01	1.0 ± 0.3
	1.00 ± 0.01	1.63 ± 0.02	1.6 ± 0.1
Block surfactant	0.60	2.53 ± 0.02	1.6 ± 0.3
	1.19	2.64 ± 0.02	3.1 ± 0.3

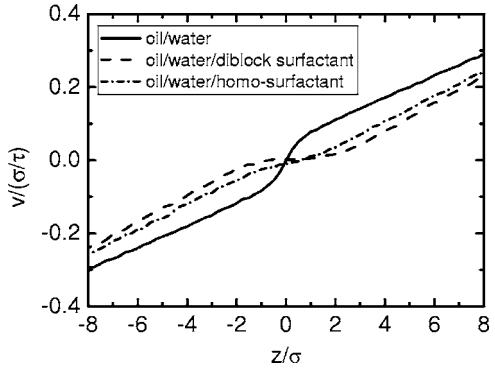

FIG. 4. Velocity profiles of oil-water, oil-water-homosurfactant, and oil-water-diblock surfactant systems under shear. The results are for a planar interface.

ity at the interface increases compared to the bulk value while a stick interface refers to that the slope of velocity at the interface decreases compared to the bulk value. Figure 4 shows the velocity profiles for oil-water system, oil-water-homosurfactant system and oil-water-diblock surfactant system under shear. In the absence of surfactant, a clear slip is observed for pure oil-water system with a slip length $S=3.22\pm0.04\sigma$. The addition of surfactant, changes the "slip" to a "stick" behavior. In Table II we show the effect of both the low and the high surface coverage of surfactants on the interfacial behavior. In all cases stick interfaces are observed. Our results clearly show that both the adsorbed amount and the structure of surfactants affect the stick length. However, diblock surfactants are much more effective at enhancing the momentum transfer across the interface. This is due to a much larger extension of diblock surfacants into both phases at same surface coverage (Table II). We note that during the simulation we observe that while homosurfactants desorb from the drop surface, block surfactants never desorb. This indicates that block surfactants need much larger shear to remove them and as a result should contribute more to the stress transfer across the interface. However, we cannot extract any quantitative information about this effect on drop deformation. Therefore, when we compare the exchange kinetics effect to the much clearer correlation of stress transfer with the extension of the surfactant layer into the water phase, we believe the exchange kinetics is at best a secondary effect.

The ability of the surfactant layer to improve the stress transfer across the interface also effects the point at which the drop will break up. While a slip interface (no surfactants) is a result of a lower interfacial viscosity (when compared to the bulk), a stick interface results from a higher interfacial viscosity. This implies that though the adsorbed surfactant increases the deformation ratio of a drop due to reduction of slip, it also increases the critical deformation ratio for breakup due to an increase in the effective viscosity of the drop. In other words, the increase in the critical deformation ratio necessary for break up that we observed for the soluble block surfactant covered drop could be a result of the enhanced interfacial viscosity of the drop.

Our simulations show that local effects resulting from changes in the architecture of the surfactant molecules can result in behavior that cannot be predicted using continuum theories. As the system size becomes comparable to the size of the interfacial layer, a limit that is being rapidly approached in emerging micro/nano-fluidic techniques, these local effects will dominate and it will become increasingly important to account for molecular phenomena in order to model the system accurately.

We gratefully acknowledge funding from the Mitsubishi Chemical Corporation, Japan. We would also like to thank Professors Wu and Shnidman for useful discussions.

[1] H. A. Stone, Annu. Rev. Fluid Mech. **26**, 65 (1994).
[2] B. J. Briscoe, C. J. Lawrence, and W. G. P. Mietus, Adv. Colloid Interface Sci. **81**, 1 (1999).
[3] D. Langevin, Adv. Colloid Interface Sci. **88**, 209 (2000).
[4] H. A. Stone and L. G. Leal, J. Fluid Mech. **220**, 161 (1990).
[5] Y. Pawar and K. J. Stebe, Phys. Fluids **8**, 1738 (1996).
[6] X. F. Li and C. Pozrikidis, J. Fluid Mech. **341**, 165 (1997).
[7] W. J. Milliken and L. G. Leal, J. Colloid Interface Sci. **166**, 275 (1994).
[8] C. D. Eggleton and K. J. Stebe, J. Colloid Interface Sci. **208**, 68 (1998).
[9] S. Velankar, P. Van Puyvelde, J. Mewis, and P. Moldenaers, J. Rheol. **45**, 1007 (2001).
[10] P. Walstra, Chem. Eng. Sci. **48**, 333 (1993).
[11] E. H. Lucasssen-Reynders and K. A. Kuijpers, Colloids Surf. **65**, 175 (1992).
[12] A. Williams, J. J. M. Janssen, and A. Prine, Colloids Surf., A **125**, 189 (1997).
[13] J. J. M. Janssen, A. Boon, and W. G. M. Agterof, AIChE J. **40**, 1929 (1994).
[14] L. Levitt and C. W. Macosko, Macromolecules **32**, 6270 (1999).
[15] J. Koplik and J. R. Banavar, Phys. Fluids A **5**, 521 (1993).
[16] G. S. Grest and K. Kremer, Phys. Rev. A **33**, 3628 (1986).
[17] Y. Lyatskaya *et al.*, J. Phys. Chem. **100**, 1449 (1996).
[18] For instance, in experimental work [13], $\gamma/\gamma_0=0.25-1.0$, $\theta_0/\theta_0(\infty)=0.04-0.9$ [where θ_0 and $\theta_0(\infty)$ are the surfactant surface concentration and saturated surfactant surface concentration, respectively], $Ca>0.4$, and *Pe* is O(4000) as estimated from the bulk diffusion constant. Continuum calculations [4,6], have used *Pe* ranging from O(0.01) to O(100) and *Ca* up to 0.5.
[19] G. I. Taylor, Proc. R. Soc. London, Ser. A **146**, 501 (1934).
[20] J. M. Rallison, J. Fluid Mech. **109**, 465 (1981).
[21] C. Creton, E. J. Kramer, C. Y. Hui, and H. R. Brown, Macromolecules **25**, 3075 (1992).
[22] C. Yeung, A. C. Balazs, and D. Jasnow, Macromolecules **25**, 1357 (1992).
[23] J. Stecki and S. Toxvaerd, J. Chem. Phys. **103**, 4352 (1995).